

# Information content of the non-linear power spectrum: the effect of beat-coupling to large scales

Christopher D. Rimes<sup>1</sup>\* and Andrew J. S. Hamilton<sup>1,2</sup>\*

<sup>1</sup>JILA, University of Colorado, 440 UCB, Boulder, CO 80309-0440, U.S.A.

<sup>2</sup>Department of Astrophysical and Planetary Sciences, University of Colorado, 391 UCB, Boulder, CO 80309-0391, U.S.A.

Submitted to Monthly Notices of the Royal Astronomical Society  
arXiv:astro-ph/0511418v1 14 Nov 2005

## ABSTRACT

We measure the information contained in the non-linear matter power spectrum about the amplitude of initial, linear power from an ensemble of periodic  $N$ -body simulations using two methods. The first is the traditional ensemble method, in which the covariance of power is estimated from the scatter over many random realizations. The second uses a novel technique to measure the covariance matrix from each simulation individually by re-weighting the density field with a carefully chosen set of weighting functions. The two methods agree at linear scales, but unexpectedly they disagree substantially at increasingly non-linear scales. Moreover, the covariance of non-linear power measured using the re-weightings method changes with box size. The numerical results are consistent with an explanation given in a companion paper, which argues that the cause of the discrepancy is beat-coupling, in which products of Fourier modes separated by a small wavevector couple by gravitational growth to the large-scale beat mode between them. In real galaxy surveys, the covariance of power at non-linear scales is likely to be dominated by beat-coupling to the largest scales of the survey. We confirm the result of a previous paper, that at translinear scales the power spectrum contains little information over and above that in the linear power spectrum, but that there is a marked increase in information at non-linear scales. However, because of beat-coupling, only part of the information potentially available at non-linear scales is actually measurable from real galaxy surveys.

**Key words:** cosmology: theory – large-scale structure of Universe.

## 1 INTRODUCTION

Recent progress in cosmological parameter estimation has been characterized by rapid convergence of constraints from a wealth of different types of observations – galaxy clustering, the Lyman- $\alpha$  forest power spectrum, galaxy cluster abundances, high-redshift type Ia supernovae, weak gravitational lensing, big-bang nucleosynthesis and many others – towards a single, well-determined ‘concordance’ cosmological model. Of particular importance has been the combination of high precision maps of anisotropies in the cosmic microwave background (CMB) with measurements of galaxy clustering from large redshift surveys, which yield complementary constraints on key cosmological parameters (e.g. Efstathiou et al. 2002; Spergel et al. 2003; Tegmark et al. 2004; Seljak et al. 2005; Sanchez et al. 2005).

Galaxy clustering analyses (e.g. Percival et al. 2001; Tegmark et al. 2004; Cole et al. 2005; Eisenstein et al. 2005) are generally restricted to scales  $\gtrsim 20 h^{-1}$  Mpc, where den-

sity fluctuations are still linear, galaxy-matter bias appears to be independent of scale (although it does depend on luminosity and on galaxy type) and the matter power spectrum directly traces the spectrum of density fluctuations at recombination. At smaller scales, where much of the observational data in galaxy surveys lie, the extent to which the linear power spectrum can be recovered from the non-linear power spectrum remains unknown. Non-linear evolution changes the shape of the power spectrum in a non-trivial way, and introduces broad correlations between measurements of power at different wavenumbers (Meiksin & White 1999; Scoccimarro, Zaldarriaga & Hui 1999; Cooray & Hu 2001). The early success of analytic formalisms at producing invertible one-to-one mappings between linear and non-linear spectra (Hamilton et al. 1991; Peacock & Dodds 1994, 1996) suggested that information in the linear power spectrum may be preserved into the non-linear regime, but other work (Meiksin, White & Peacock 1999; Seo & Eisenstein 2005) has shown that non-linear evolution erases features in the power spectrum, perhaps leading to an irreversible loss of information.

\* E-mail: rimes@colorado.edu, Andrew.Hamilton@colorado.edu

In an earlier letter (Rimes & Hamilton 2005, hereafter Paper I), we reported measurements of the amount of information in the non-linear power spectrum about the amplitude of the linear power spectrum for the currently favoured (concordance) cosmological model, from a large ensemble of  $N$ -body simulations. We found that there exists little independent information in the translinear regime ( $k \simeq 0.2\text{--}0.8 h \text{ Mpc}^{-1}$  at the present day) over and above that in the linear power spectrum, but that in the fully non-linear regime there appears to be a significant amount of information beyond that measurable from the linear power spectrum.

Measuring the information content of the non-linear power spectrum involves measuring the covariance matrix of non-linear power, which, if determined as in Paper I from the scatter over an ensemble, requires performing a large number of  $N$ -body simulations. This is costly in terms of computing time, especially if the simulations are of high quality. In an attempt to reduce the computational overhead and to streamline the measurement of information, we devised a new technique, described in detail in a companion paper (Hamilton, Rimes & Scoccimarro 2005, hereafter HRS), for estimating the covariance of power from individual simulations, by re-weighting the density field using a set of carefully chosen windows.

In the present paper, we use the re-weighting technique to measure the amount of information in the non-linear power spectrum, for the same set of simulations used in Paper I. We compare the results to those obtained with the ensemble method and present a number of tests of the method.

Unexpectedly, we find that, far from agreeing, the covariance of power measured by the re-weightings method substantially exceeds that measured by the ensemble method. When we first encountered this discrepancy, it seemed to us that it must be caused by a ‘bug’ in our code, and we performed numerous numerical tests to track it down. Belatedly, we realized that the discrepancy was caused not by a bug but by a real physical process, which we term ‘beat-coupling’. The physical origin of beat-coupling is described by HRS, who illustrate its effects with examples using perturbation theory and the hierarchical model.

This paper is organized as follows. In Section 2 we set out our definition of information, and discuss the decorrelation choices that must be made to allocate information to prescribed wavebands. This section also provides a more detailed exposition of the techniques employed in Paper I. Section 3 describes the numerical simulations used in both this paper and the previous one. Section 4 compares measurements of the covariance of power using both ensemble and re-weightings methods, and describes several tests of the results. In Section 5 we compare the information content of the non-linear power spectrum, measured using the two different methods. Our conclusions are summarized in Section 6.

## 2 INFORMATION

### 2.1 Fisher information

The Fisher information matrix is defined (e.g. Tegmark, Taylor & Heavens 1997) as

$$F^{\alpha\beta} \equiv - \left\langle \frac{\partial^2 \ln \mathcal{L}}{\partial p_\alpha \partial p_\beta} \right\rangle, \quad (1)$$

where  $\mathcal{L}(p_\alpha | \text{data})$  is the likelihood function – the multivariate probability distribution of the model parameters  $p_\alpha$  given the available data and a set of model assumptions (the Bayesian prior). Fisher information is additive over independent measurements, clearly a desirable property for information to possess. Its importance in parameter estimation is encapsulated in the Cramér-Rao inequality, which limits the maximum precision with which a single parameter  $p_\alpha$  can be measured to

$$\langle \Delta \hat{p}_\alpha^2 \rangle \geq 1/F_{\alpha\alpha}, \quad (2)$$

if the estimator  $\hat{p}_\alpha$  is unbiased and if this is the only parameter being estimated from the data. Here and throughout this paper we use hats to distinguish an *estimate* of a quantity from its true value. If estimates of the parameters are Gaussian distributed about their expectation values – a good approximation in the limit of a large amount of data, thanks to the central limit theorem – then their covariance matrix is well-approximated by the inverse of the Fisher matrix:

$$\langle \Delta \hat{p}_\alpha \Delta \hat{p}_\beta \rangle \simeq (F^{-1})_{\alpha\beta}. \quad (3)$$

### 2.2 Power spectrum

We consider a statistically homogeneous and isotropic density field  $\rho(\mathbf{r})$ . The power spectrum  $P(k)$  of density fluctuations of such a field is defined by

$$\langle \delta_{\mathbf{k}} \delta_{\mathbf{k}'} \rangle = (2\pi)^3 \delta_{3D}(\mathbf{k} + \mathbf{k}') P(k), \quad (4)$$

where  $\delta_{\mathbf{k}}$  is the Fourier transform of the overdensity  $\delta(\mathbf{r}) \equiv \rho(\mathbf{r})/\bar{\rho} - 1$  and  $\delta_{3D}(\mathbf{k})$  is a 3-dimensional Dirac delta function. Statistical isotropy requires that the power spectrum be a function only of the magnitude  $k \equiv |\mathbf{k}|$  of the wavevector  $\mathbf{k}$ .

For Gaussian fluctuations, each  $\delta_{\mathbf{k}}$  has real and imaginary components that are independently Gaussianly distributed with variance  $P(k)/2$ . Usually, power is estimated by averaging over shells in Fourier space. For Gaussian fluctuations, the expected covariance matrix of shell-averaged estimates of power is diagonal, with variance

$$\langle \Delta \hat{P}(k) \rangle = 2P(k)^2/N_k, \quad (5)$$

where  $N_k$  is the number of modes in the shell around  $k$  (a finite number in the case of a realistic galaxy survey or a periodic  $N$ -body simulation). Here  $\delta_{\mathbf{k}}$  and its complex conjugate  $\delta_{-\mathbf{k}}$  are counted as contributing two distinct modes, the real and imaginary parts of  $\delta_{\mathbf{k}}$ .

### 2.3 Information in the power spectrum

Here, as in Paper I, we measure the Fisher information  $I$  in a single parameter: the log of the amplitude  $A$  of the initial (post-recombination) matter power spectrum, that is,

$$I \equiv - \left\langle \frac{\partial^2 \ln \mathcal{L}}{\partial \ln A^2} \right\rangle. \quad (6)$$

For Gaussian density fluctuations, the power spectrum completely specifies the statistical properties of the density field, so that the only explicit dependence of the likelihood  $\mathcal{L}$  is

on the power spectrum. For non-Gaussian fluctuations, the likelihood function may also depend explicitly on other parameters. However, as in Paper I, we consider only the information contained in the power spectrum  $P(k)$ , in which case the information  $I$  defined by equation (6) can be expanded as

$$I = - \left\langle \sum_{k,k'} \frac{\partial \ln P(k)}{\partial \ln A} \frac{\partial^2 \ln \mathcal{L}}{\partial \ln P(k) \partial \ln P(k')} \frac{\partial \ln P(k')}{\partial \ln A} \right\rangle. \quad (7)$$

The middle term on the right-hand side of equation (7) is the Hessian of the vector  $\ln P(k)$  of log non-linear powers, the expectation value of which is the Fisher matrix. The power spectrum  $P(k)$  is averaged over spherical shells in  $k$ -space; a typical shell in the non-linear regime contains several thousand to hundreds of thousands of distinct Fourier modes, so it is reasonable to invoke the central limit theorem to assert that estimates of power will be Gaussianly distributed about their expectation values. This assertion holds even if the density field is itself non-Gaussian. We test this is explicitly in Section 4.2.3. In the Gaussian approximation, the Hessian in equation (7) can be approximated by the inverse of the covariance matrix of estimates of log-power.

The remaining terms in equation (7) are two partial derivatives which describe the sensitivity of the non-linear power to changes in the amplitude  $A$  of the initial linear power. In the linear regime these derivatives are identically unity, since  $P_L(k) \propto A$ ; at non-linear scales they are equal to the growth rate of the non-linear power spectrum relative to the linear, which can be conveniently measured from simulations.

The information  $I$  has a particularly simple interpretation for Gaussian fluctuations. Following equation (5), it is equal to half the total number  $N$  of Gaussian modes:

$$I = N/2. \quad (8)$$

As was found in Paper I and is confirmed in Section 5 of the present paper, the information in the non-linear power spectrum  $P(k)$  is significantly less than the information in the linear power spectrum at the same wavenumber. This decrease in information could result from a transfer of information from larger to smaller scales, a diversion of information into other quantities (such as the bispectrum), or an irreversible loss of information.

#### 2.4 Decorrelated band powers

The quantity  $I$  defined by equation (7) is the total amount of information contained in the non-linear power spectrum about the parameter  $\ln A$ . Some of this information is degenerate between measurements of power at different wavenumbers as a result of the broad correlations introduced by non-linear evolution.

Hamilton & Tegmark (2000) showed how to decorrelate a power spectrum by defining a set of uncorrelated band-power estimates:

$$\frac{\hat{B}_k}{P_k} = \sum_{k'} W_{kk'} \frac{\hat{P}_{k'}}{P_{k'}}, \quad (9)$$

where we use the index notation  $P_k = P(k)$  to emphasize the fact that the shell-averaged power spectrum  $P(k)$  can be

viewed as a discrete vector in Fourier space. Decorrelation is the process of assigning shared information uniquely to a given wavenumber. The band-power windows  $W_{kk'}$  in equation (9) are elements of a decorrelation matrix, each column of the matrix being a discrete window for one band-power  $B_k$ . There are many (actually an infinite number) of schemes for decorrelating the power spectrum, corresponding to different ways of sharing out degenerate information between wave bands. The reader is directed to Hamilton & Tegmark (2000) for a discussion of the relative merits of selected decorrelation schemes.

Both sides of equation (9) are scaled by  $P_k$ , which is a fiducial power spectrum. This scaling ensures that a given band power  $B_k$  is not dominated by leakage from wavenumbers  $k'$  where the window is small but  $P_{k'}$  is large. The choice  $P_k = \langle \hat{P}_k \rangle$  guarantees that the expectation value of the windowed band power estimates at each wavenumber is equal to the original power spectrum, provided that the windows are suitably normalized:

$$\sum_{k'} W_{kk'} = 1. \quad (10)$$

We experimented with various decorrelation matrices, eventually opting for the upper triangular matrix  $\mathbf{U}$  obtained from a generalized form of the Cholesky decomposition of the Fisher matrix  $\mathbf{F}$  of the scaled power spectrum:

$$\mathbf{U}^\top \mathbf{\Lambda} \mathbf{U} = \mathbf{F}, \quad (11)$$

where  $\mathbf{\Lambda}$  is a diagonal matrix – the Fisher matrix of the scaled, decorrelated band powers. In the central-limit-theorem approximation that estimates of power are Gaussianly distributed, the Fisher matrix  $\mathbf{F}$  is approximately equal to the scaled inverse covariance of power:

$$\mathbf{F} \simeq \mathbf{P} \langle \Delta \hat{\mathbf{P}} \Delta \hat{\mathbf{P}}^\top \rangle^{-1} \mathbf{P}^\top. \quad (12)$$

Here,  $\mathbf{P}$  is a diagonal matrix whose non-zero elements are equal to the fiducial power spectrum  $P_k$ . Mathematically, upper Cholesky decorrelation is equivalent to taking a matrix composed of all the elements of the covariance matrix up to some wavenumber  $k_{\max}$ , inverting this matrix, and summing all the elements of the resulting Fisher matrix to arrive at a measure of the accumulated information  $I(\leq k_{\max})$  up to that wavenumber.

Upper Cholesky decorrelation yields band-power windows that are highly asymmetric, with the band power at each wavenumber  $k$  containing contributions only from power on larger scales. A problem with the other schemes that we tried (including the square root of the scaled Fisher matrix, recommended by Hamilton & Tegmark 2000), is that there is an appreciable covariance between large, linear scales and small, non-linear scales. Applying anything other than upper Cholesky decorrelation assigns some of this covariance to large scales, causing the information at linear scales to depart from the expected Gaussian information, equation (5).

While there is a certain arbitrariness about choosing upper Cholesky decorrelation over other possibilities, the resulting cumulative information  $I(\leq k_{\max})$  has the virtue of a simple interpretation: it is the information in the power spectrum  $P(k)$  at wavenumbers  $k \leq k_{\max}$ , uncontaminated by information in power at smaller scales.

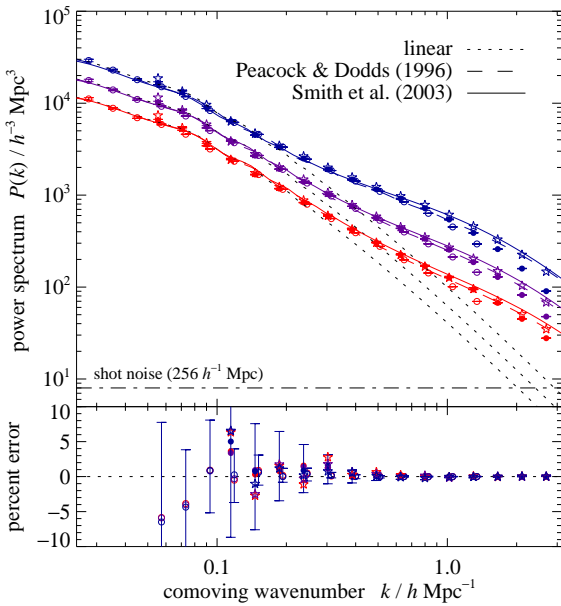


**Figure 1.** Evolution of the non-linear power spectrum. Top panel: mean power spectrum from the  $256 h^{-1} \text{ Mpc}$  PM simulations (open points, with error bars derived from the scatter between individual simulations); the  $128 h^{-1} \text{ Mpc}$  PM simulations (filled points with error bars); and the  $128 h^{-1} \text{ Mpc}$  ART simulations (stars). Power spectra are shown for three epochs (bottom to top:  $a = 0.5, 0.67$  and  $1$ ). The linear power spectrum is shown by the dotted curves in each panel. The solid and dashed curves are, respectively, from the fitting formulae of Smith et al. (2003) and Peacock & Dodds (1996). The dot-dashed line marks the level of the shot noise in the  $256 h^{-1} \text{ Mpc}$  simulations; the shot noise in the  $128 h^{-1} \text{ Mpc}$  simulations is a factor of 8 lower. Bottom panel: deviation between the mean power spectra of weighted densities and the power spectrum of the unweighted density. The points are medians from 100 of the PM simulations of each box size and the 25 ART simulations at the same 3 epochs. Error bars mark the upper and lower quartiles of the distribution.

Because the Fisher matrix of the uncorrelated band powers  $B(k) = B_k$  is by definition diagonal, equation (7) reduces to a sum over a single wavenumber and the cumulative information is:

$$I(\leq k) = - \left\langle \sum_{k=0}^{k_{\max}} \frac{\partial \ln B(k)}{\partial \ln A} \frac{\partial^2 \ln \mathcal{L}}{\partial \ln B(k)^2} \frac{\partial \ln B(k)}{\partial \ln A} \right\rangle. \quad (13)$$

### 3 SIMULATIONS

The simulations used in this paper are the same as those used in Paper I. The main ensemble comprises 600 gravitational  $N$ -body simulations of the concordance cosmological model: 400 simulations with a box size of  $256 h^{-1} \text{ Mpc}$  and a further 200 with a box size of  $128 h^{-1} \text{ Mpc}$ . These simulations were evolved using a particle-mesh (PM) code with  $128^3$  dark matter particles and a  $256^3$  force mesh.

An additional 25 simulations, also with a box size of  $128 h^{-1} \text{ Mpc}$ , were run using a parallel version of the adaptive mesh refinement (AMR) code ART

(Kravtsov, Klypin & Khokhlov 1997). Alone, this is an insufficient number to give precise statistics, but together with the much larger ensemble of PM simulations, the ART simulations serve as a useful check of our results on small scales, where the AMR technique is more accurate. For the ART simulations, we used  $128^3$  particles and a  $128^3$  root mesh with, at most, three levels of refinement, giving a maximum spatial resolution equivalent to that of a  $1024^3$  mesh in dense regions. Gaussian initial conditions for the ART simulations were set up using the publicly available GRAFIC package.

The cosmological parameters adopted are those of Tegmark et al. (2004, second-last column of their table 4):

$$(\Omega_M, \Omega_\Lambda, f_b, h, \sigma_8) = (0.29, 0.71, 0.16, 0.71, 0.97) \quad (14)$$

This choice of parameters gives the best fit to the combination of the power spectrum of fluctuations in the cosmic microwave background as measured by the Wilkinson Microwave Anisotropy Probe (WMAP) and galaxy clustering as measured by the Sloan Digital Sky Survey (SDSS), under the important assumptions (among others) of a spatially flat universe ( $\Omega_k = 0$ ) with a cosmological constant ( $w = -1$ ) and a scale-invariant primordial power spectrum ( $n_s = 1$ ). Each simulation was seeded with a different, randomly chosen realization of a Gaussian random field with a power spectrum corresponding to the above cosmological model. The matter transfer function was calculated from the fitting formula of Eisenstein & Hu (1998) for universes with a significant baryon content.

The non-linear power spectra of the above simulations are plotted in Fig. 1 for three epochs:  $a = 0.5, 0.67$  and  $1.0$ , with error bars showing the scatter between individual realizations. Power spectra were calculated by Fourier transforming the weighted density field on a single  $256^3$  grid<sup>1</sup>. The resulting power spectra were corrected for smoothing by dividing by the square of the Fourier transform of the mass assignment window, prior to subtracting the shot noise contribution (Smith et al. 2003). As is to be expected, the power in the PM simulations falls significantly below that measured in the higher resolution ART simulations at small scales, as a result of mesh effects in the PM simulations. The power spectrum from the ART simulations, on the other hand, agrees well with the fits to previous  $N$ -body simulations by Peacock & Dodds (1996) and Smith et al. (2003) at the scales of interest. We restrict our analyses to scales for which corrections to power from particle-cell assignment are small, and the shot noise sub-dominant, so uncertainties in both of these corrections should not affect our results.

In what follows, where the results from the  $128 h^{-1} \text{ Mpc}$  PM and ART simulations are consistent, we combine them into a single data set for clarity.

<sup>1</sup> ‘Chaining’ (Jenkins et al. 1998), a clever way to extend measurements of the power spectrum to smaller scales by superposing the eight octants of a periodic cube on to a single octant, unfortunately cannot be applied to the measurement of covariance, because it involves a reduction in the number of Fourier modes. For Gaussian fluctuations, each mode is independent, so each folding reduces the number of modes by a constant factor 8. At non-linear scales, however, adjacent modes are highly correlated, so subsampling them by a factor of 8 does not reduce the effective number of modes correspondingly.

## 4 CONSTRUCTING THE COVARIANCE MATRIX

Estimating the amount of information in a set of measurements requires knowledge of their covariance matrix. The most direct way to measure the covariance of estimates of the power spectrum is to run an ensemble of  $N$ -body simulations, each having a different, random realization of the initial density field (e.g. Meiksin & White 1999; Scoccimarro et al. 1999; Paper I) – a computationally expensive endeavour because many hundreds of realizations are required to yield an accurate estimate of the covariance matrix (Meiksin & White 1999; Paper I).

Alternative approaches to measuring covariances include ‘jackknife’, in which ensembles are formed by removing selected data from the original sample, and ‘bootstrap’, in which ensembles are formed by resampling with replacement (Künsch 1989). These methods work provided that the data being sampled comprise independent random variables drawn from the same distribution. For correlated data, Künsch (1989) suggested an extension to the bootstrap approach, in which the data are first split into blocks whose length is larger than the characteristic length of the correlations, and these blocks are then re-sampled to generate the bootstrap sample. In early experiments, we tried a form of ‘block bootstrap’ in which we filled each octant of a simulation cube with a block of data selected randomly from the cube. Unfortunately, the method did not work well. The sharp edges of the octants introduced spurious small-scale power, and the covariance of small-scale power differed substantially from that measured by the ensemble method. The mathematical relation between the covariance of power obtained by the block bootstrap method and the true covariance of power is sufficiently obscure that it was difficult to assess the possible causes of the discrepancy.

In HRS, we argue that all variations on jackknife and bootstrap are really just different ways of re-weighting the data to yield a new estimate of the quantity of interest, and that the best way to avoid unpleasant side-effects on spatial data is to re-weight with a smooth function of position. Further, by re-weighting the simulation with a function that contains only large-scale Fourier modes, unpleasant numerical artefacts in the power spectrum are confined to the largest scales, making them much easier to deal with.

### 4.1 Covariance of power of weighted density

Following HRS, we define the  $i$ 'th weighted density by

$$\rho_i(\mathbf{r}) \equiv w_i(\mathbf{r})\rho(\mathbf{r}). \quad (15)$$

We use the minimum variance set of weightings recommended in section 3 of HRS. In real space the  $i$ 'th weighting has the form

$$w_i(\mathbf{r}) = \sqrt{2} \cos \left[ 2\pi \left( \mathbf{k}_i \cdot \mathbf{r} + \frac{1}{16} \right) \right], \quad (16)$$

where

$$\mathbf{k}_i = \begin{cases} \{1, 0, 0\} & 12 \text{ weightings} \\ \{1, 1, 0\} & 24 \text{ weightings} \\ \{1, 1, 1\} & 16 \text{ weightings} \end{cases} \quad (17)$$

The different weightings are obtained by all possible reflections and rotations of the components of  $\mathbf{k}$ , which yields

26 weightings in total, allowing for all of the symmetries in equation (16). A further 26 weightings are obtained by adding a phase shift of  $\pi/2$ , i.e.  $1/16 \rightarrow 5/16$  in equation (16), equivalent to translating one of the coordinates by a quarter box (because of the symmetry of the weighting functions, only one such translation yields a distinct weighting). The estimate of power from this second set of weightings is predicted by HRS to be highly anti-correlated with that obtained from the first set of 26 weightings, but they are sufficiently uncorrelated that including all 52 weightings does yield a better measurement of the covariance matrix than is obtained from only 26 weightings. It is possible to apply more weightings constructed from higher order modes than those in equation (17) but, as argued in section 3.5 of HRS, these contain progressively less independent information, and yield progressively less accurate estimates of covariance.

A covariance matrix estimated as the average of  $n$  distinct estimates can have a rank no greater than  $n$ , a fact also pointed out recently by (Pan & Szapudi 2005). The 52 weightings given by equation (17) prove sufficient to yield, for each simulation, a non-singular (no zero eigenvalues), and indeed positive definite (no negative eigenvalues) estimate of the covariance matrix for the 20 bins of wavenumber used here.

As a practical matter, we implement the re-weighting scheme by weighting individual particles, before assigning the density to the Fourier mesh. The weighted overdensity at point  $j$  on the mesh is defined to be

$$\delta_i(\mathbf{r}_j) \equiv \frac{\rho_i(\mathbf{r}_j)}{\bar{\rho}} - 1, \quad (18)$$

where  $\bar{\rho}$  is the mean of the *unweighted* density field. Note that this is a different convention to that used in HRS, in which the quantity being transformed is

$$\Delta\rho_i(\mathbf{r}) \equiv \rho_i(\mathbf{r}) - \bar{\rho}_i(\mathbf{r}), \quad (19)$$

where  $\bar{\rho}_i(\mathbf{r}) = w_i(\mathbf{r})$  and  $\bar{\rho} \equiv 1$ . The difference between these two conventions only affects the power on the largest scales (those wavebands containing modes appearing in equation 17) and can most easily (and accurately) be corrected for in Fourier space. However, since the covariance on these scales is not correctly reproduced by the re-weighting method, we simply exclude them from our analyses.

The covariance of power over the ensemble of weighted powers is related to the true covariance of power by (HRS)

$$\langle \Delta\hat{P}(k)\Delta\hat{P}(k') \rangle = 2\langle \Delta\hat{P}_i(k)\Delta\hat{P}_i(k') \rangle_i, \quad (20)$$

where  $\langle \dots \rangle_i$  denotes an average over different weightings and the factor 2 corrects the covariance of the ensemble to the true covariance of estimates of power. The deviation  $\Delta\hat{P}_i(k)$  in the power spectrum of the  $i$ 'th weighted density must be measured relative to some expected or mean value, and HRS discussed two possibilities. The first is to measure the deviation relative to the power spectrum of the unweighted density of the simulation:

$$\Delta\hat{P}_i(k) \equiv \hat{P}_i(k) - \hat{P}(k). \quad (21)$$

The second is to measure the deviation relative to the mean of the power spectra of the weighted densities:

$$\Delta\hat{P}_i(k) \equiv \hat{P}_i(k) - \frac{1}{N} \sum_i \hat{P}_i(k). \quad (22)$$

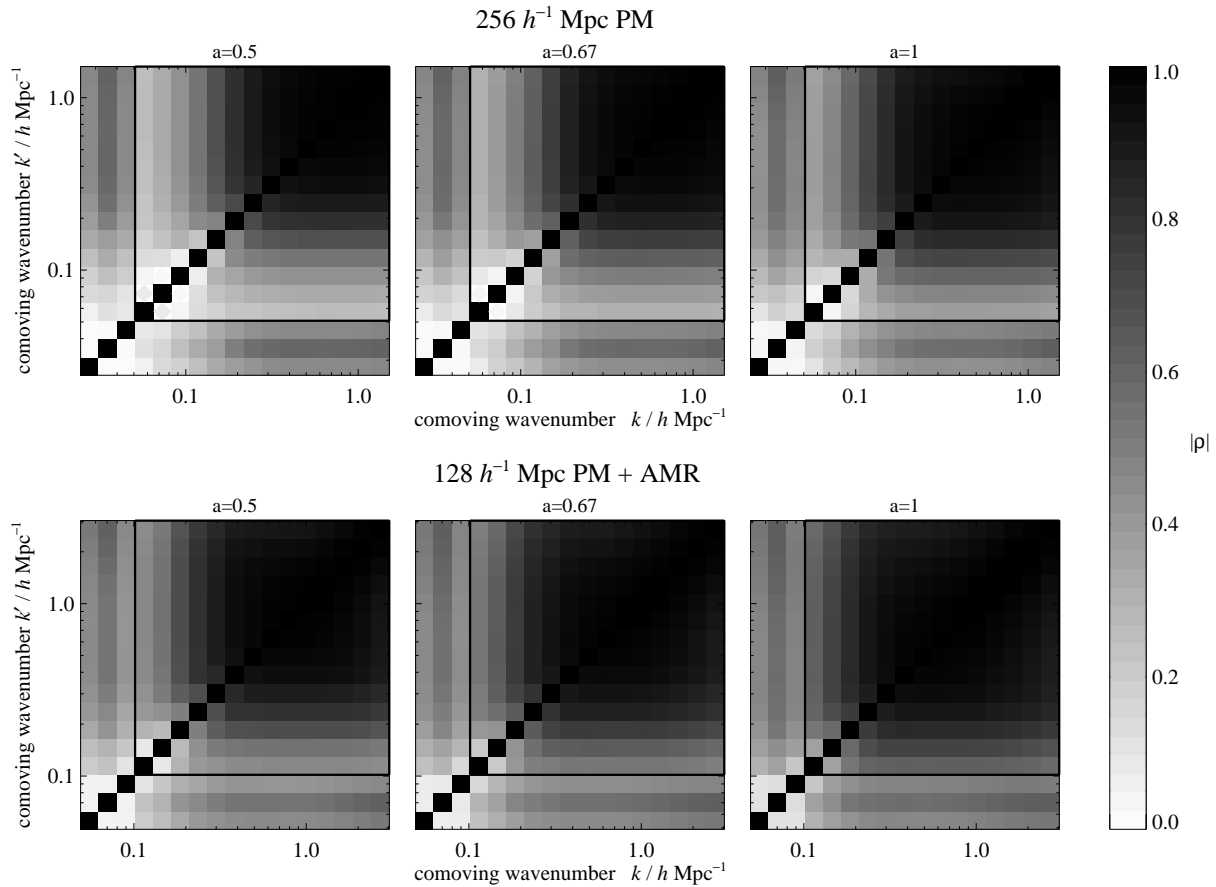


**Figure 2.** Correlation matrices of estimates of non-linear power using the re-weighting scheme of HRS at 3 epochs (left to right  $a = 0.5, 0.67$  and  $1$ ). Correlation matrices were estimated separately for each simulation and then averaged over simulations. Results shown are averages over 100 PM simulations of each box size and additionally, in the case of the  $128 h^{-1}$  Mpc boxes, the 25 ART simulations. Positive correlations are shown by completely filled bins while diamonds denote anti-correlations. Greyscale is used to indicate the magnitude of the correlations, ranging from 0 (no correlation) to 1 (perfect correlation). A heavy, black border outlines the region of each covariance matrix that is unaffected by numerical artefacts from the re-weighting scheme. Bins outside of the bordered area are excluded from further analyses.

The advantage of the first strategy, equation (21), is that the power spectrum of the unweighted density is, by symmetry, the most accurate estimate of power in a simulation, so the statistical uncertainty is potentially least in this case. However, the power spectra of weighted densities are likely to be slightly biased relative to the power spectrum of the unweighted density, because weighting the density effectively smooths the power, which biases it if power is other than a linear function of wavenumber. The advantage of the second strategy, equation (22), is that it removes this slight bias, so the systematic uncertainty is potentially smaller in this case.

The lower panel of Fig. 1 shows the median and quartiles of the distribution of the deviations between the averaged power spectra of weighted densities and the power spectrum of the unweighted density of each simulation (c.f. equation 20 of HRS). The two agree well on small scales, but on larger scales they can differ by up to 20 percent in extreme cases.

In the following sections, we show results for both strategies, equations (21) and (22), and find that the two strategies give consistent results. However, we do find that equation (21) gives variances that are slightly but system-

atically higher than those from equation (22), which we attribute to the systematic bias between the power spectra of weighted densities versus the power spectrum of the unweighted density. For the purposes of computing information, Section 5, we therefore choose the second strategy, equation (22).

Each set of weightings in equation (17) is generated from a different wavenumber  $k_i = |\mathbf{k}_i|$ , so we expect estimates of power from each set to be biased in a slightly different way. This bias is small; nevertheless it is preferable to estimate the covariance matrix separately from each set of weightings and then combine them to obtain a single estimate of the covariance matrix, weighting by the number of weightings in each set. This is the procedure that we adopt in Section 5.

## 4.2 Tests

In this section we describe several tests of the measurement of covariance of power. In Section 4.2.1 we show that the weightings and ensemble methods give consistent results for the correlation coefficients of band-powers. By contrast, in

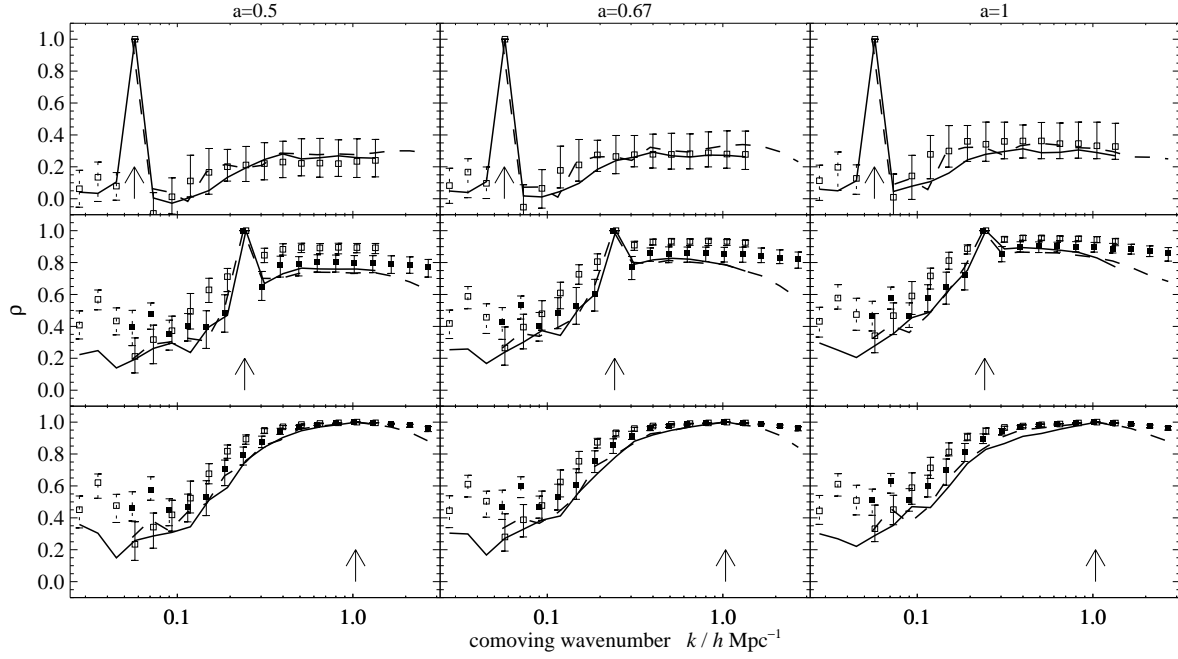


**Figure 3.** Correlations between estimates of the non-linear power spectrum using the re-weighting method, with  $\Delta P_i$  defined by equation (22). The three columns show cross-sections through the correlation matrices at 3 epochs (left to right  $a = 0.5, 0.67$  and  $1$ ), while each row shows a cross-section at a different wavenumber ( $k' = 0.057, 0.242$  and  $1.036 h Mpc^{-1}$ ), marked by the vertical arrow in each panel. Symbols with error bars mark the median and quartiles of the distribution of correlation co-efficients measured from each individual simulation for the  $256 h^{-1} Mpc$  PM (open symbols) and  $128 h^{-1} Mpc$  PM+ART (filled symbols) simulations. Dotted error bars are used for points that are outside of the range of wavenumbers for which the covariance is expected to be reliably estimated by the re-weighting method. Solid and dashed lines show the correlations between (unweighted) estimates of power using the full ensemble of  $256 h^{-1} Mpc$  PM and  $128 h^{-1} Mpc$  PM+ART simulations, respectively. Data for the  $128 h^{-1} Mpc$  boxes are missing in the top row because this entire cross-section lies outside the reliable region for this box size.

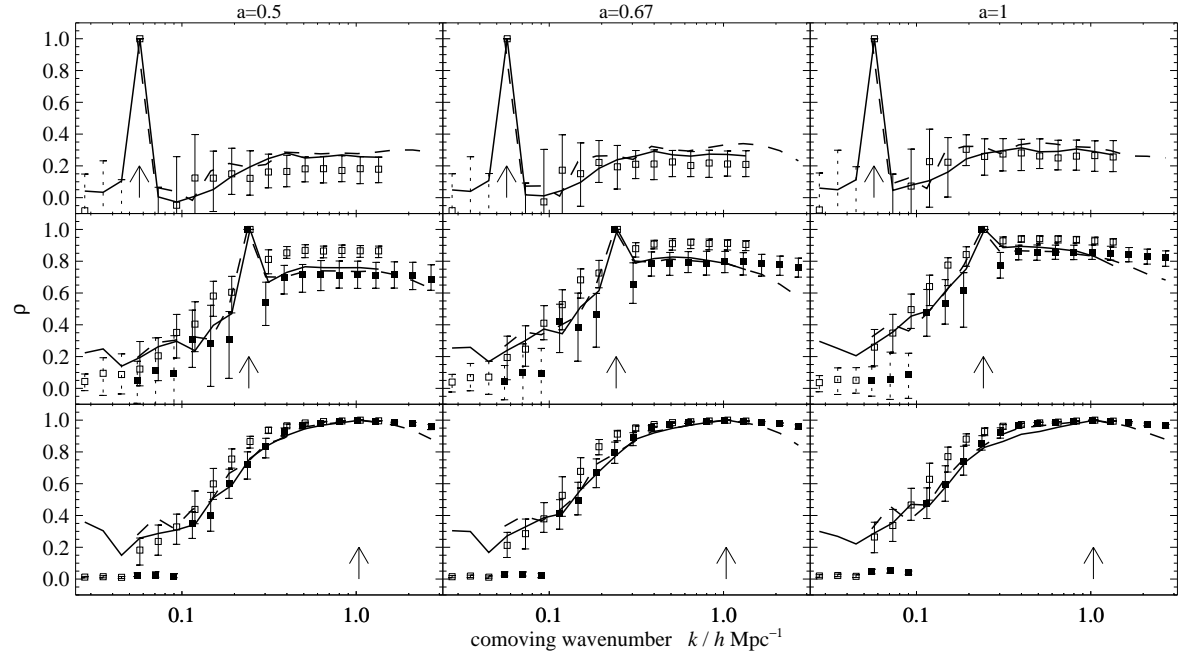


**Figure 4.** As Fig. 3, but with  $\Delta P_i$  defined by equation (21). The symbols and lines have the same meanings as in Fig. 3. Together, the two figures demonstrate that the different methods give broadly consistent results.

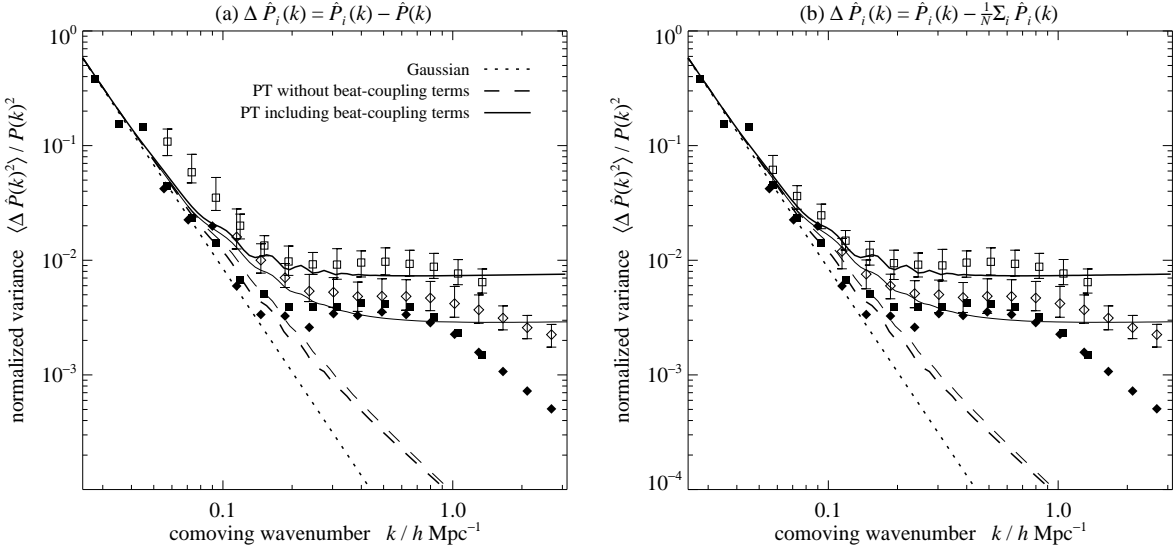


**Figure 5.** Variance of estimates of power using the re-weighting method with  $\Delta P_i$  defined by (a) equation (22) and (b) equation (21). Open symbols show the variance, normalized to the square of the power, at  $a = 1$  in the  $256 h^{-1}$  Mpc simulations (squares) and the  $128 h^{-1}$  Mpc simulations (diamonds). The results for the  $128 h^{-1}$  Mpc box size have been shifted vertically by a factor 8 to compensate for the reduced density of modes and enable direct comparison between the two box sizes. Error bars mark the upper and lower quartiles of the distribution of estimates of variance over individual simulations. Solid symbols give the corresponding results measured using the ensemble method (these points are the same in both panels). The solid and dashed curves are predictions from perturbation theory, both with (solid) and without (dashed) the beat-coupling terms (see HRS for details of the calculation). The heavier lines are the results for the  $256 h^{-1}$  Mpc box size. The dotted line is the expected variance for Gaussian fluctuations.

Section 4.2.2 we show that the two methods give substantially different results for the variance of power at non-linear scales. In Section 4.2.3 we check the assumption that the distribution of estimates of power is (thanks to the central limit theorem) adequately Gaussian.

#### 4.2.1 Correlations in the power spectrum

Fig. 2 shows the matrix of correlation coefficients,

$$\rho_{kk'} \equiv \frac{\langle \Delta P_k \Delta P_{k'} \rangle}{\sqrt{\langle (\Delta P_k)^2 \rangle \langle (\Delta P_{k'})^2 \rangle}}, \quad (23)$$

of estimates of the non-linear power spectrum at three epochs, measured using the re-weighting scheme outlined in Section 4.1. Each matrix is the average result from 100 individual PM simulations and, in the case of the  $128 h^{-1}$  Mpc boxes, 25 ART simulations. The final epoch ( $a = 1$ ) can be directly compared to fig. 2 of Paper I, in which we show the results from the ensemble method. We expect numerical artefacts from the re-weighting to be restricted to wavenumbers  $k \leq \sqrt{3}k_b$ , the highest wavenumber used in the weighting functions. Fig. 2 shows that this is indeed the case: the degree of correlation changes abruptly between bins containing wavenumbers inside and outside this limit. In the following analysis, we use only bins with wavenumbers a factor of 2 away from the fundamental mode of the box,  $k \geq 2k_b$ .

Fig. 3 shows three cross-sections through each of the correlation matrices in Fig. 2. The data plotted are the medians and quartiles of the distribution over the independent realizations. The measurements from the re-weighting and ensemble methods are generally consistent, although the re-weighting method tends to yield somewhat higher correla-

tions at smaller scales, and higher for the  $256 h^{-1}$  Mpc boxes than the  $128 h^{-1}$  Mpc boxes. The scatter between individual simulations is considerable, especially where the correlation coefficient is small.

Fig. 4 shows the same results, but with the deviations  $\Delta \hat{P}_i(k)$  in the power spectra of weighted densities being measured relative to the power spectrum of the unweighted density, equation (21), as opposed to the mean of the power spectra of weighted densities, equation (22). The correlation coefficients are similar to those shown in Figure 3, as they should be.

#### 4.2.2 Variance of the power spectrum

While the re-weighting and ensemble methods yield consistent results for the correlation matrix of non-linear power, the variance of (and hence the information contained in) the non-linear power spectrum is an altogether different matter.

Fig. 5 shows the variance, normalized to the square of the unweighted power spectrum, estimated using the re-weighting method. We show results for both equation (21) and equation (22). Notice that, as expected, equation (21) overestimates the variance of power on large scales. On small scales, however, the results are entirely consistent.

For Gaussian fluctuations, the normalized variance equals  $2/N_k$  (equation 5), where  $N_k$  is the number of modes in a given wavenumber bin. For a periodic box, the number of modes in a set of logarithmically-spaced bins increases with central wavenumber as  $N_k \propto k^3$ . The  $128 h^{-1}$  Mpc simulations have fewer modes (by a factor of 8) at a given wavenumber, so the results for this box size have been shifted vertically down by this factor to allow a direct comparison

between the results for the two box sizes. As in Fig. 3, the data shown in Fig. 5 are medians over many individual simulations, with error bars marking the quartiles of the distribution. The results for the  $128 h^{-1}$  Mpc PM simulations and the  $128 h^{-1}$  Mpc ART simulations are consistent, so we combine them into a single set of points for clarity (a figure showing the ART results alone appears as fig. 2 of HRS).

The two different box sizes yield consistent results when the ensemble method is used. For the re-weighting method, on the other hand, there are clear discrepancies, both between the re-weighting method and the ensemble method and between the two box sizes. At translinear and non-linear scales, the variance measured by re-weighting is significantly higher than that measured for the ensemble, particularly for the larger box size, and the discrepancy grows ever larger at smaller scales.

Fig. 5 also shows the predictions of perturbation theory. The calculation of these curves is described in section 4.3 of HRS. Perturbation theory helps to explain the discrepancies both between the results of the ensemble and re-weighting methods, and between the two different box sizes. The variance measured by the re-weighting technique departs from the ensemble result where the (constant) beat-coupling term (equation 94 of HRS) becomes the dominant source of variance. The source of this term – coupling of closely-spaced Fourier modes to the large-scale beat mode between them – is discussed in section 4 of HRS. The magnitude of the beat-coupling term is proportional to the amplitude of the power spectrum on roughly the size of the box, which explains why different sizes of simulation box yield systematically different estimates of the small-scale variance. Perturbation theory correctly predicts the magnitude of the discrepancy between the small-scale variance estimated from the two different sizes of simulation.

Note that perturbation theory fails to reproduce the correct non-linear variance for the ensemble method (dashed lines). This is simply a result of the theory breaking down in the highly non-linear regime, and may also be responsible for the relatively small discrepancies between the results of the re-weighting method and the theoretical curves in Fig. 5.

#### 4.2.3 Distribution of estimates of power

In Section 2 we asserted that, thanks to the central limit theorem, estimates of power should be Gaussianly distributed about their expectation value, even in the highly non-linear regime. Since our analysis relies on the validity of this assumption it is worth putting to the test.

Fig. 6 shows the distribution of deviations of estimates of power using both the re-weighting method and the ensemble method for wavenumbers in the non-linear regime (which we take to be  $k > 0.2 h^{-1}$  Mpc). Individual histograms for each waveband have been scaled to unit variance and stacked to produce a single distribution for each method. The estimates of power from the re-weighted simulations are indeed distributed close to Gaussianly. Assuming Poisson statistics, the value of  $\chi^2$  for the fit is 5.84 per degree of freedom, which seems reasonable, given the high degree of correlation between estimates of non-linear power. For the ensemble method, the distribution is also close to Gaussian, although there are deviations from Gaussianity – in particular the presence of a sharper than Gaussian peak and a tail

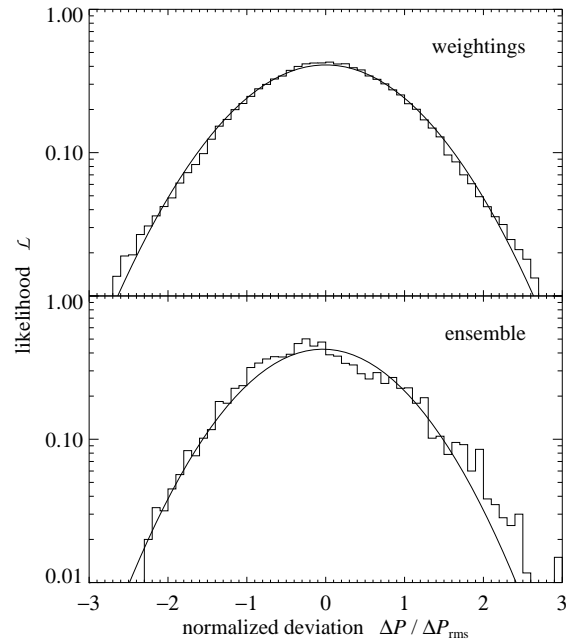


**Figure 6.** Distributions of estimates of non-linear power, equation (22), using the re-weighting method (top panel) and the ensemble method (bottom panel). Individual histograms for all bands with wavenumbers  $k > 0.2 h^{-1}$  Mpc, containing at least 2000 Fourier modes, are scaled to unit variance and stacked. The smooth curves are Gaussian fits to the data, assuming Poisson weighting of the counts in each bin.

of large, positive deviations that cause the actual mean and variance of power to be slightly larger than the fitted values. The value of  $\chi^2$  in this case is 3.86 per degree of freedom, for Poisson statistics.

## 5 INFORMATION CONTENT OF THE NON-LINEAR POWER SPECTRUM

In the previous section, we showed that measuring the covariance of non-linear power by re-weighting an individual simulation yields substantially different results at non-linear scales than is found from the scatter over an ensemble of simulations. The discrepancy is consistent with the explanation proposed by HRS: beat-coupling between the covariance on non-linear scales and the power on large scales. The difference in covariance between the two methods translates directly into a difference in the quantity of information in the non-linear power spectrum.

Which method is correct? The answer is that it depends on what one is trying to measure. In Paper I we were interested in the question: does non-linear evolution conserve information? The ensemble method measures covariances between the amplitudes of Fourier modes with precisely defined (delta function) wavenumbers. If information is conserved by non-linear evolution then it is this quantity that, overall, remains invariant with time.

The re-weighting method, on the other hand, is more directly applicable to a realistic, finite galaxy survey. It measures the amount of information that is actually extractable

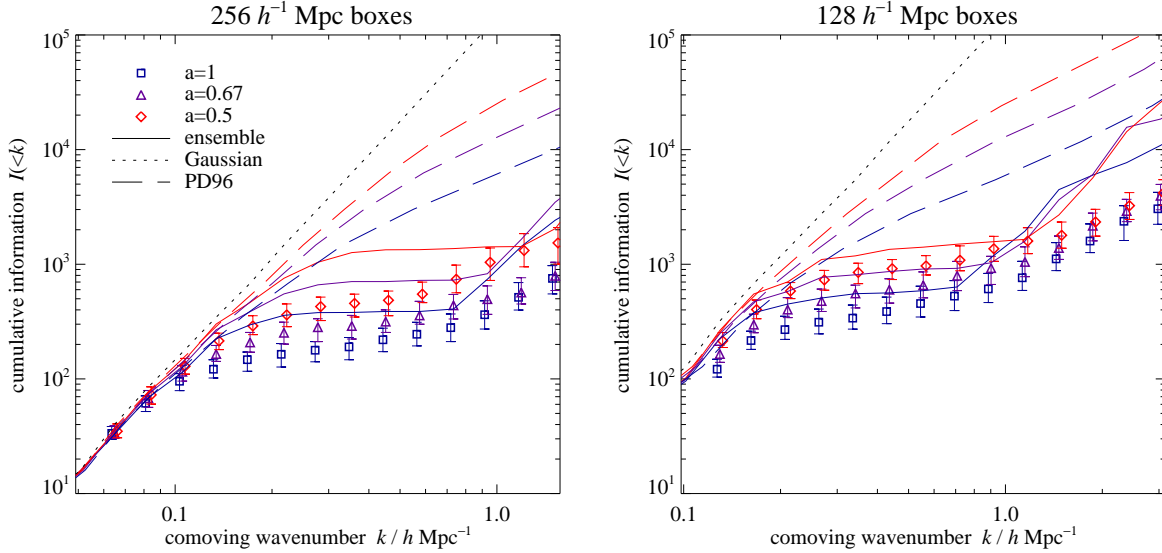


**Figure 7.** Cumulative information in the non-linear power spectrum at 3 epochs (top to bottom:  $a = 0.5, 0.67$  and  $1$ ). Points with error bars are medians and quartiles of the results measured using the re-weighting method on (left panel) 100 PM simulations with a box size of  $256 h^{-1}$  Mpc and (right panel) 100 PM simulations and 25 ART simulations with a box size of  $128 h^{-1}$  Mpc. For clarity, the three sets of points have been artificially separated by a small factor in wavenumber, with the  $a = 0.67$  points having the correct wavenumber. The results for the  $128 h^{-1}$  Mpc box size have been shifted vertically by a factor 8 to compensate for the reduced number of modes and enable direct comparison between the two box sizes. Solid lines are the same quantity measured using the ensemble method. The dotted line marks the expected amount of information for Gaussian fluctuations and the dashed curves are the result of applying the PD96 scaling to the dotted line at each epoch.

from such a survey. This turns out to depend on the amplitude of the power spectrum on the scale of the survey. As we show in the following sections, the amount of information recoverable in practice from the non-linear power spectrum is significantly less than what is in theory contained therein. Beat-coupling of small-scale fluctuations to the power on the largest scales in the survey limits how much information can be extracted from a finite galaxy survey.

In Paper I, we used covariance matrices measured from the ensemble of simulations to estimate the amount of information contained in the non-linear power spectrum about  $\ln A$ , the log of the amplitude of the initial power spectrum (equation 7). In the following sections of the present paper, we compare our previous results with measurements of the same quantity for covariance matrices estimated using the re-weighting method.

### 5.1 Method

We decorrelate the power spectrum of each simulation individually, using the covariance matrix estimated using the re-weighting method. As our fiducial power spectrum  $P_k$  in equation (9) we use the true (unweighted) power in each simulation. The re-weighting method restricts the range of wavenumbers for which the covariance matrix – and hence the Fisher information – can be reliably measured to  $k > \sqrt{3}k_b$ . Since our purpose is to measure the *cumulative* information, equation (13), up to some wavenumber  $k_{\max}$ , the contribution from wavenumbers smaller than this limit must be taken into account. For the  $256 h^{-1}$  Mpc boxes we assume that the excluded bins contain the expected amount of information for Gaussian fluctuations ( $N_k/2$ , where  $N_k$  is

the number of Fourier modes in those bins). That this is a reasonable assumption is confirmed by the fact that the first few bins for which we do have measurements of the variance using the re-weighting method follow the Gaussian expectation closely (see the top panel of Fig. 5). For the  $128 h^{-1}$  Mpc boxes there is a further complication. The lower limit on the wavenumbers accessible using the re-weighting method brings us into the regime in which non-linear effects start to become important. The most reasonable thing to do here would seem to be to use the results from the  $256 h^{-1}$  Mpc boxes to estimate the quantity of missing information. Although there are clearly systematic differences between the results of the re-weighting method for different box sizes, these are small at the scales in question.

## 5.2 Results

### 5.2.1 Ensemble method

Fig. 7 shows the cumulative information as a function of wavenumber at 3 epochs ( $a = 0.5, 0.67$  and  $1$ ), for both methods of estimating the covariance of power. For the re-weighting method we show the median and quartiles of the distribution of results from the individual simulations.

As discussed in Paper I, the ensemble method yields very little independent information in the translinear regime ( $k \simeq 0.2-0.8 h^{-1}$  Mpc), over and above that in the linear regime. At smaller scales, however, there is a sudden upturn in the cumulative information, implying that the power spectrum at fully non-linear scales contains unique information about the amplitude of the initial power spectrum, that is not found in the present day linear power spectrum.

In Paper I, we interpreted the decrease in information

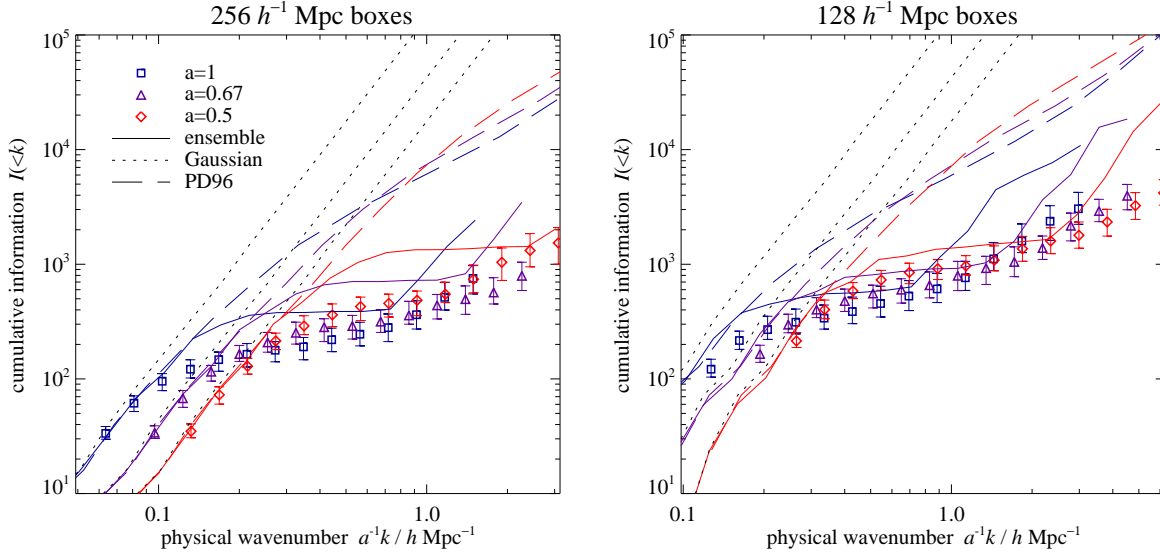


**Figure 8.** Cumulative information, as Fig. 7, plotted as a function of physical (rather than comoving) wavenumber. The symbols and lines have the same meanings as in Fig. 7, but note the expanded range of the horizontal axis.

in the translinear regime as the result of rapid transfer of information from larger to smaller scales. An alternative explanation, which was mentioned in Paper I but discarded as being contrived, is that information is temporarily diverted into higher order statistics, such as the bispectrum, in the translinear regime. Since filamentary structures are more readily described by higher-order statistics than by the power spectrum alone, it is entirely plausible that, on translinear scales, the bispectrum does contain information not present in the power spectrum, about the initial conditions of structure formation, and that this information is somehow returned to the power spectrum on smaller scales.

We argued in Paper I that, if information is conserved overall then, under the assumption of stable clustering, the amount of information up to a given physical (as opposed to comoving) wavenumber ought to be independent of time in the fully non-linear regime. Fig. 8 shows the cumulative information, plotted as a function of physical wavenumber  $k/a$ , for the same 3 epochs as in Fig. 7. For the ensemble method, the results are consistent with the hypothesis that information is largely conserved by non-linear evolution.

### 5.2.2 Re-weighting method

Qualitatively, the behaviour of the cumulative information – as a function of both wavenumber and cosmic epoch – for the re-weighting method is consistent with that for the ensemble method. The flattening in the translinear regime, followed by an upturn at small scales is preserved. There are, however, clear quantitative differences. Overall, the information measured using the re-weighting method is considerably less than when the ensemble method is used. Beat-coupling to large scales prevents much of the information that is, in principle, contained in the power spectrum from being extracted when the re-weighting method is used.

As predicted by perturbation theory, the beat-coupling contribution to the covariance, which is a factor  $\sim P(2k_b)/P(k)$  larger than the other terms at a given  $k$ ,

becomes increasingly dominant at smaller scales. For the power spectrum considered here, the contribution from beat-coupling also increases with cosmic epoch. We would therefore not expect the cumulative information, measured using the re-weighting method, up to a given physical wavenumber to be necessarily constant over time, even in the stable clustering regime. However, the time dependence turns out to be weak and Fig. 8 is not inconsistent with information being conserved overall.

### 5.3 Relevance to observations

As argued by HRS, beat-coupling affects real galaxy surveys. Beat-coupling contributions to the covariance of power occur whenever Fourier modes have a finite width, as opposed to being delta-functions at discrete wavevectors. The effect of beat-coupling is greatest when the largest scales in a survey are close to the peak of the power spectrum (approximately  $400 h^{-1} \text{ Mpc}$  comoving;  $k \simeq 0.016 h \text{ Mpc}^{-1}$ ). The covariance of power in real galaxy surveys is likely to be dominated by beat-coupling on small scales and, counter-intuitively, to be sensitive to the power on the largest scales of the survey.

The results of Section 5.2.1 suggest that the amount of information extractable in practice from the non-linear power spectrum of a realistic, finite galaxy survey is likely to be significantly less than the amount that is theoretically present in the power spectrum.

## 6 SUMMARY

This paper extends and expands on the results reported in Paper I concerning the Fisher information contained in the non-linear power spectrum about the amplitude of the initial (post-recombination) linear power.

In Paper I, we measured the covariance of power by the traditional ensemble method, that is, from the scatter

in power over a large ensemble of simulations. Here we reported measurements of covariance of power from both the ensemble method and a new method, described in a companion paper (HRS), in which smoothly varying weighting functions are applied to each simulation to yield a separate estimate of the covariance of power for each simulation.

We have shown that the two methods yield substantially different estimates for the covariance of power at non-linear scales. This does not mean, however, that one or other of the methods is incorrect. Rather, it turns out that measuring the covariance of power is a more subtle problem than we had previously suspected. Beat-coupling – the process whereby the covariance between Fourier modes separated by a small wavevector couple by gravitational growth to the large-scale beat mode between them – dominates the covariance on non-linear scales. We compared our results to a calculation using perturbation theory (HRS) and found that the theory explains qualitatively the features of beat-coupling, seen in the simulations.

The effects discussed in this paper have direct relevance to real galaxy surveys. Our results show that the information extractable from the power spectrum of a galaxy survey is likely to be considerably less than the amount of information in principle contained therein. The cause of this loss of information is beat-coupling of small scale fluctuations to the power on the largest scales in the survey.

## ACKNOWLEDGEMENTS

We are grateful to Anatoly Klypin and Andrey Kravtsov for making the MPI implementation of ART available to us and for help with its application. We also thank Nick Gnedin, Mathias Zaldarriaga and Román Scoccimarro for useful discussions. This work was supported by NSF grant AST-0205981 and by NASA ATP award NAG5-10763. GRAFIC is part of the COSMICS package, which was developed by Edmund Bertschinger under NSF grant AST-9318185. Some of the simulations used in this work were performed at the San Diego Supercomputer Center using resources provided by the National Partnership for Advanced Computational Infrastructure under NSF cooperative agreement ACI-9619020.

## REFERENCES

Cole S., et al., 2005, MNRAS, p. 681  
 Cooray A., Hu W., 2001, ApJ, 554, 56  
 Efstathiou G., et al., 2002, MNRAS, 330, L29  
 Eisenstein D. J., et al., 2005, ApJ, 633, 560  
 Eisenstein D. J., Hu W., 1998, ApJ, 496, 605  
 Hamilton A. J. S., Kumar P., Lu E., Matthews A., 1991, ApJ, 374, L1  
 Hamilton A. J. S., Rimes C. D., Scoccimarro R., 2005, MNRAS (submitted)  
 Hamilton A. J. S., Tegmark M., 2000, MNRAS, 312, 285  
 Jenkins A., et al., 1998, ApJ, 499, 20  
 Kravtsov A. V., Klypin A. A., Khokhlov A. M., 1997, ApJS, 111, 73  
 Künsch A. R., 1989, Ann. Stat., 17, 1217  
 Meiksin A., White M., 1999, MNRAS, 308, 1179  
 Meiksin A., White M., Peacock J. A., 1999, MNRAS, 304, 851  
 Pan J., Szapudi I., 2005, MNRAS, 362, 1363  
 Peacock J. A., Dodds S. J., 1994, MNRAS, 267, 1020  
 Peacock J. A., Dodds S. J., 1996, MNRAS, 280, L19  
 Percival W. J., et al., 2001, MNRAS, 327, 1297  
 Rimes C. D., Hamilton A. J. S., 2005, MNRAS, 360, L82  
 Sanchez A., Baugh C. M., Percival W. J., Peacock J. A., Padilla N. D., Cole S., Frenk C. S., Norberg P., 2005, MNRAS, submitted (astro-ph/0507583)  
 Scoccimarro R., Zaldarriaga M., Hui L., 1999, ApJ, 527, 1  
 Seljak U., et al., 2005, Phys. Rev. D, 71, 103515  
 Seo H.-J., Eisenstein D. J., 2005, ApJ, 633, 575  
 Smith R. E., et al., 2003, MNRAS, 341, 1311  
 Spergel D. N., et al., 2003, ApJS, 148, 175  
 Tegmark M., et al., 2004, Phys. Rev. D, 69, 103501  
 Tegmark M., Taylor A. N., Heavens A. F., 1997, ApJ, 480, 22

This paper has been typeset from a **TeX/ L<sup>A</sup>T<sub>E</sub>X** file prepared by the author.